Journal of Research in Pharmacy
Research Article
www.jrespharm.com

Development and Assessment of Mitoxantrone and 4-Methyl Umbelliferone Nanoemulsions for Chemotherapeutic Potential on MCF-7 Cell Line

Vineeta MEENA [1], Rajani MATHUR[2], Azka GULL[1], Neha JAIN[1], Dhruv KUMAR[3], Satyendra KUMAR RAJPUT[4], Swati MADAN[1]*

1 Amity Institute of Pharmacy, Amity University, Noida, Uttar Pradesh
2 Delhi Institute of Pharmaceutical Education and Research, New Delhi.
3 Amity Institute of Molecular Medicine and Stem Cell Research, Amity University, Noida, Uttar Pradesh
4 Gurukula Kangri Vishwavidyalaya, Department of Pharmaceutical Sciences, Haridwar, Uttarakhand, India
* Corresponding Author. E-mail: smadan3@amity.com (S.M); Tel. +91-9891626956.

Received: 16 December 2021 / Revised: 16 March 2022 / Accepted: 18 March 2022

ABSTRACT: Every year, millions of new cases of cancer of various forms are identified, resulting in a high mortality rate. For the management of breast cancers, chemotherapeutics such as Mitoxantrone (MTO) and 4-Methyl Umbelliferone(4-MU), show significant cytotoxic effects. The goal of this research was to develop and characterize nanoemulsion of MTO and 4-MU and to further assess the cytotoxic activity of this formulation against MCF-7 cell lines using MTT assay. Aqueous microtitration technique was employed to prepare the nanoemulsion using cinnamaldehyde as an oil phase, Tween-80 as a surfactant, and PEG-400 as a co-surfactant. The developed nanoemulsions were characterized for droplet size, PDI, %transmittance, drug content, surface morphology, and in vitro release. Photomicrograph of developed NE showed spherical droplets with a mean diameter of 113.2±5.3 nm and 123.2±6.17 nm for 4-MU and MTO, respectively, and a PDI was found to be 0.254 and 0.281 for 4-MU and MTO respectively. Approximately 78.53±4.61 % of 4-MU were released under sink conditions after 8 hours in a dissolution study. MTO-NE and 4-MU-NE had a longer drug release profile in the in-vitro method when compared to standard drug solutions. The cytotoxic effect of 4-MU and 4-MU-NE was assessed on the MCF-7 cell line by MTT assay and exhibited IC50s of 3.868 mM and 1.885 Mm against MCF-7, respectively. MTO and MTO-NE had IC50s of 10.51µM and 5.027 µM against MCF-7, respectively. The results of this study show the great potential of the prepared nanoemulsions for breast cancer; hence it can be concluded that developed NEs of chemotherapeutics lead the way forward for further in-vivo research.
KEYWORDS: Mitoxantrone; 4-methyl umbelliferone; Nanoemulsion; MCF-7 cell line; MTT Assay.

1. INTRODUCTION

Breast cancer is one of the most prevalent cancers in women, and it is also the leading cause of cancer-related mortality in women (1). As for the world health organization (WHO) report in 2020, an estimated 19.3 million new cancer cases (18.1 million excluding nonmelanoma skin cancer) were diagnosed worldwide, with about 10.0 million cancer deaths (9.9 million excluding nonmelanoma skin cancer). With an expected 2.3 million new cases (11.7 percent), breast cancer has become the most diagnosed malignancy following by surpassing lung (11.4 percent), colorectal (10.0 percent), prostate (7.3 percent), and stomach (5.6 percent) cancers (2).

Breast cancer has affected 2.3 million women globally in 2020, with 685 000 fatalities. By the end of the year 2020, 7.8 million women had been diagnosed with breast cancer in the previous five years, making it the most common disease in the world. (2)

Lymph node metastases remain the most significant issue that might lead to subsequent cancer even after surgery (1)

Traditional breast cancer treatments viz surgery, chemotherapy, and radiation are effective but have several drawbacks, such as poor bioavailability and considerable side effects. Nano-drug delivery systems offer many benefits, including precise tumor targeting, high bioavailability, less adverse effects, regulated drug release, and enhanced drug solubility(3) (4).

Meena V, Mathur R, Gull A, Jain N, Kumar D, Kumar Rajput S, Madan S. Development and assessment of mitoxantrone and 4-methyl umbelliferone nanoemulsions for chemotherapeutic potential on mcf-7 cell line. J Res Pharm. 2022; 26(3): 469-482.

http://dx.doi.org/10.29228/jrp.144
ISSN: 2630-6344

Systemic toxicity substantially limits the safety and efficacy of traditional intravenous chemo- and immunotherapies. Although tremendous progress has been achieved in the domains of cancer diagnostics and biology, cancer mortality has not been improved significantly(5).

Mitoxantrone is a dihydroxy anthracene dione derivative used as a chemotherapeutic agent which is an intravenous mono- and combination therapy that has shown therapeutic effectiveness in advanced breast cancer, acute myeloid leukemia, and non-Hodgkin's lymphoma that is comparable to conventional induction and salvage treatment regimens. MTO is a Topoisomerase-II inhibitor that inhibits cell division in malignant cells by disrupting DNA repair, DNA synthesis, and DNA intercalation, as well as limiting cell proliferation and cell growth. MTO is restricted in its usage due to non-specific effects on healthy cells and tissues, as well as substantial drawbacks such as cardiotoxicity and myelosuppression (6).

Despite this, Mitoxantrone's therapeutic effectiveness is severely limited due to its high systemic toxicity and lack of specificity(7).

The malignant phenotype of numerous malignancies, notably breast cancer, is promoted by increased hyaluronan synthesis. Hyaluronic acid is involved in the migration, adhesion, and invasion of breast cancer cells(8). Breast cancer cells can also produce a variety of matrix-degrading enzymes and proinflammatory mediators as a result of HA synthesis, which is associated with tumor development.4- Methyl umbelliferone is a hyaluronic acid production inhibitor, it suppresses hyaluronan production and accumulation in the extracellular matrix as well as within breast cancer cells, particularly in those lacking the estrogen receptor.4-MU suppresses the expression of HAS2 and HYALs-1, -2, and causes the hyaluronan receptor CD44 to vanish from cell protrusions.4-MU inhibits the development of breast cancer via modulating matrix-degrading enzymes and tumor-promoting inflammatory mediators (9)

4-MU is a powerful anticancer drug that is orally bioavailable, generally nontoxic, and has anti-invasive, antiangiogenic, and perhaps anti-inflammatory effects. Because 4-MU suppresses the expression of HA receptors, HAS2 and caveolin-1, as well as Akt signaling, it may be a more effective treatment than targeting individual HA receptors. (10)

Nanoemulsions are drug delivery methods that can significantly improve the bioavailability of hydrophobic medicines while also protecting them from degradation. Because of its safety, controlled release, increased drug action and stability, selective targeting, and less toxicity, it might be very useful in delivering drugs to cancer cells (11).

The objective of the current investigation was to design and create a Nanoformulation for mitoxantrone and 4-methyl Umbelliferone that would improve drug delivery while minimizing systemic toxicity and improving specific targeting. The aim was to incorporate MTO and 4-MU in nanoemulsions and to characterize their effectiveness on MCF-7 cancer cell lines.

2. RESULTS

2.1 Preparation of calibration curve

As shown in Figure 1, the calibration curve of 4-MU and MTO was prepared using $y = 0.0078x - 0.0105$ and $y = 7.8427x - 0.0185$ at absorption maxima of 320nm and 662 nm respectively. The r^2 value of 4-MU and MTO was found to be 0.98943 and 0.99677 respectively which are close to 1 . The value of r^2 denotes that the dilutions were accurately prepared and follows Beer-lambert law.

http://dx.doi.org/10.29228/jrp.144
J Res Pharm 2022; 26(3): 469-482

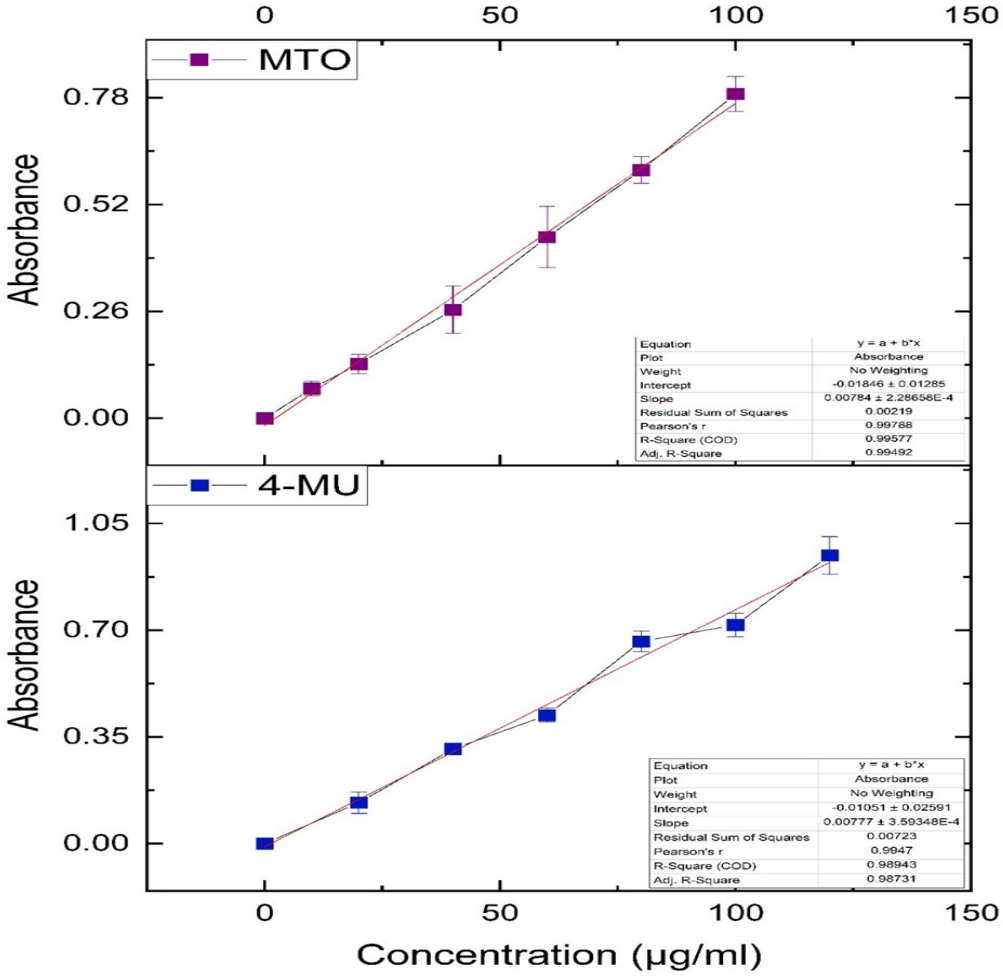

Figure 1. Calibration Plot for MTO in double distilled water at 269 nm and 4-MU in methanol and water(1:1) at 320 nm.

2.2 Screening of Excipients

Before developing the nanoemulsions, screening of excipients is a necessary step. 4-MU being lipophilic, the solubility of 4-MU in different lipids (oils) is shown in Figure 2. As per the data, 4-MU has shown significant and maximum solubility in cinnamaldehyde (83.19 mg/ml) followed by lemongrass oil (58.73 mg/ml) and so on.

http://dx.doi.org/10.29228/jrp.144
J Res Pharm 2022; 26(3): 469-482

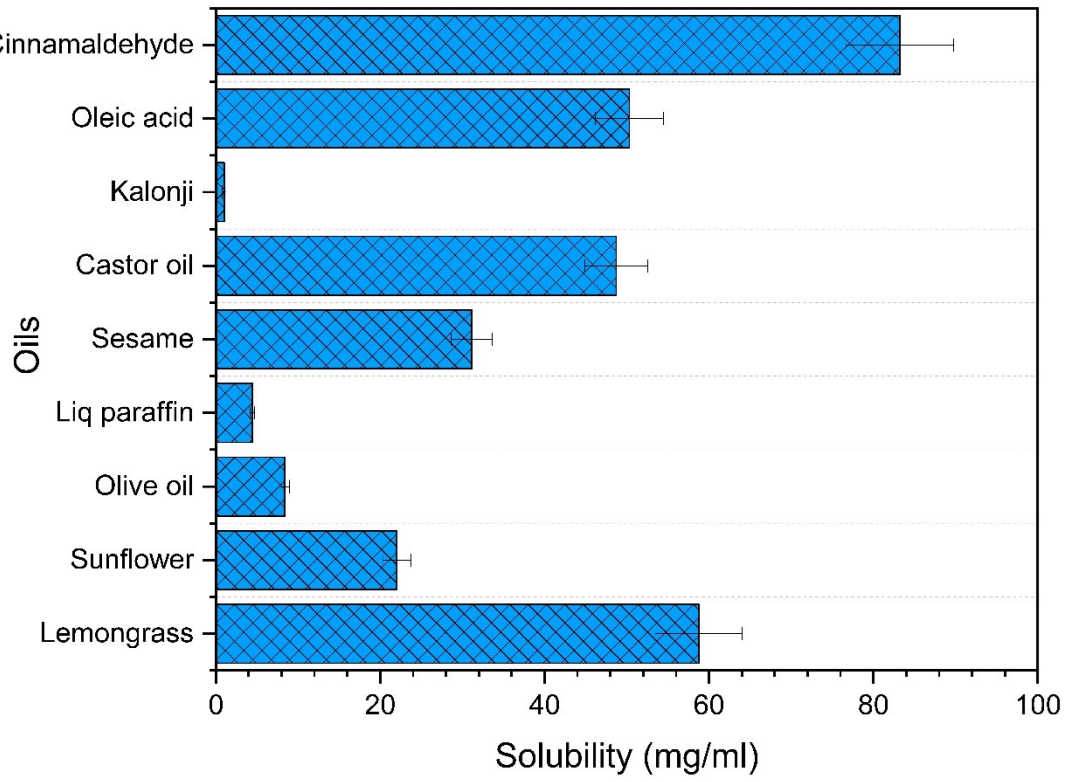

Figure 2. Solubility of 4-MU in various oils.

2.3 Screening of surfactant and cosurfactant

Nanoemulsions are thermodynamically unstable formulations. To enhance its stability, the surfactant and co-surfactant are required to be added. Surfactants form semi-stable mixtures of oil and water. The surfactant and co-surfactant ability to dissolve oil was assessed as a criterion for the selection. Figure 3 indicates that tween 80 with the highest oil solubilizing capacity of 35 µl after tween 20 µl and Peceol 19 µl respectively.

Tween-80 (HLB = 15 (6.331 mg/ml) and PEG-400 (3.13 mg/ml) were the surfactants with the highest solubilizing capability, according to the surfactants tested for solubility study. To make the S_{mix}, Tween-80 and PEG -400 were chosen as surfactant and co-surfactant.

http://dx.doi.org/10.29228/jrp.144
J Res Pharm 2022; 26(3): 469-482

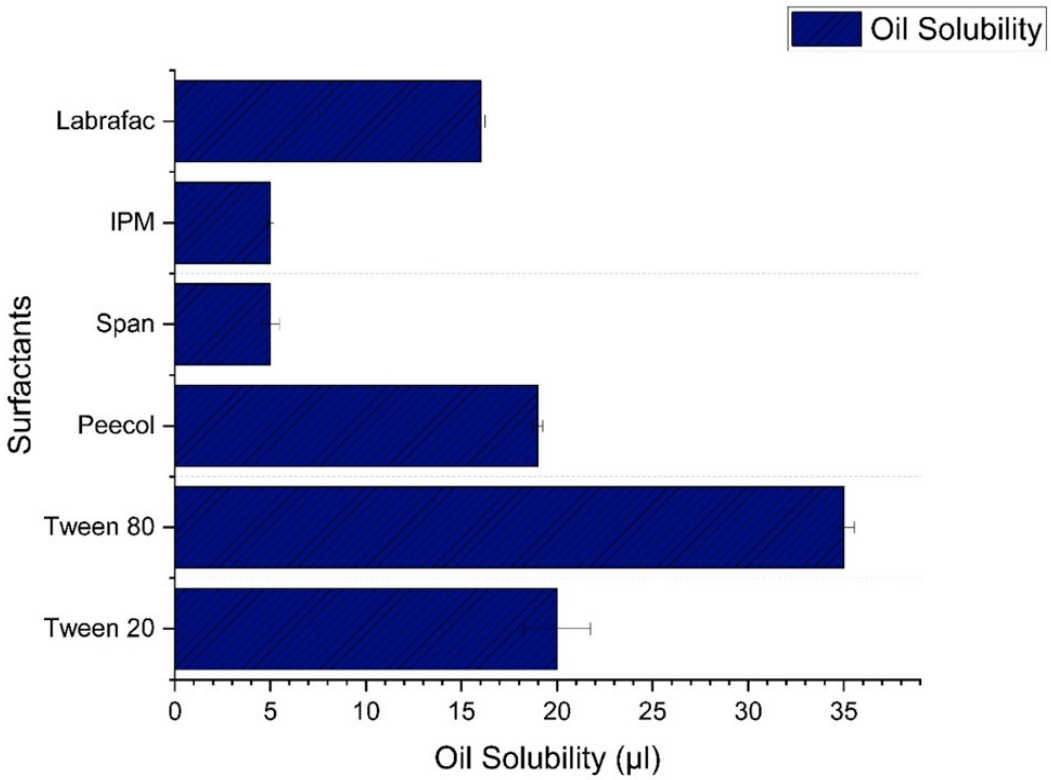

Figure 3. Oil solubilization capacity of various surfactant.

2.4 Pseudo-ternary phase diagram

The association between phase behavior of oil, water, and surfactant-cosurfactant mixture can be portrayed with the help of a phase diagram. Pseudo-ternary phase diagrams were made separately for each S_{mix} ratio to identify the regions of o/w emulsion and optimization of NE can be done.

Figure 4 illustrates different pseudo ternary phase diagrams, where colored area represents potential nanoemulsion location. It was observed that when the amount of surfactant increased with respect to the co-surfactant, the nanoemulsion region also increased. Nanoemulsion region was found to be maximum in 4:1 S_{mix} ratio whereas it was found to be minimum in 1:1. Hence. 4:1 ratio of surfactant and co-surfactant was selected.

The pseudo-ternary phase diagram not only assisted in identifying the optimal S_{mix} ratio but also in determining the minimum and maximum limit of oil and S_{mix}.

http://dx.doi.org/10.29228/jrp.144
J Res Pharm 2022; 26(3): 469-482

Journal of Research in Pharmacy
Research Article

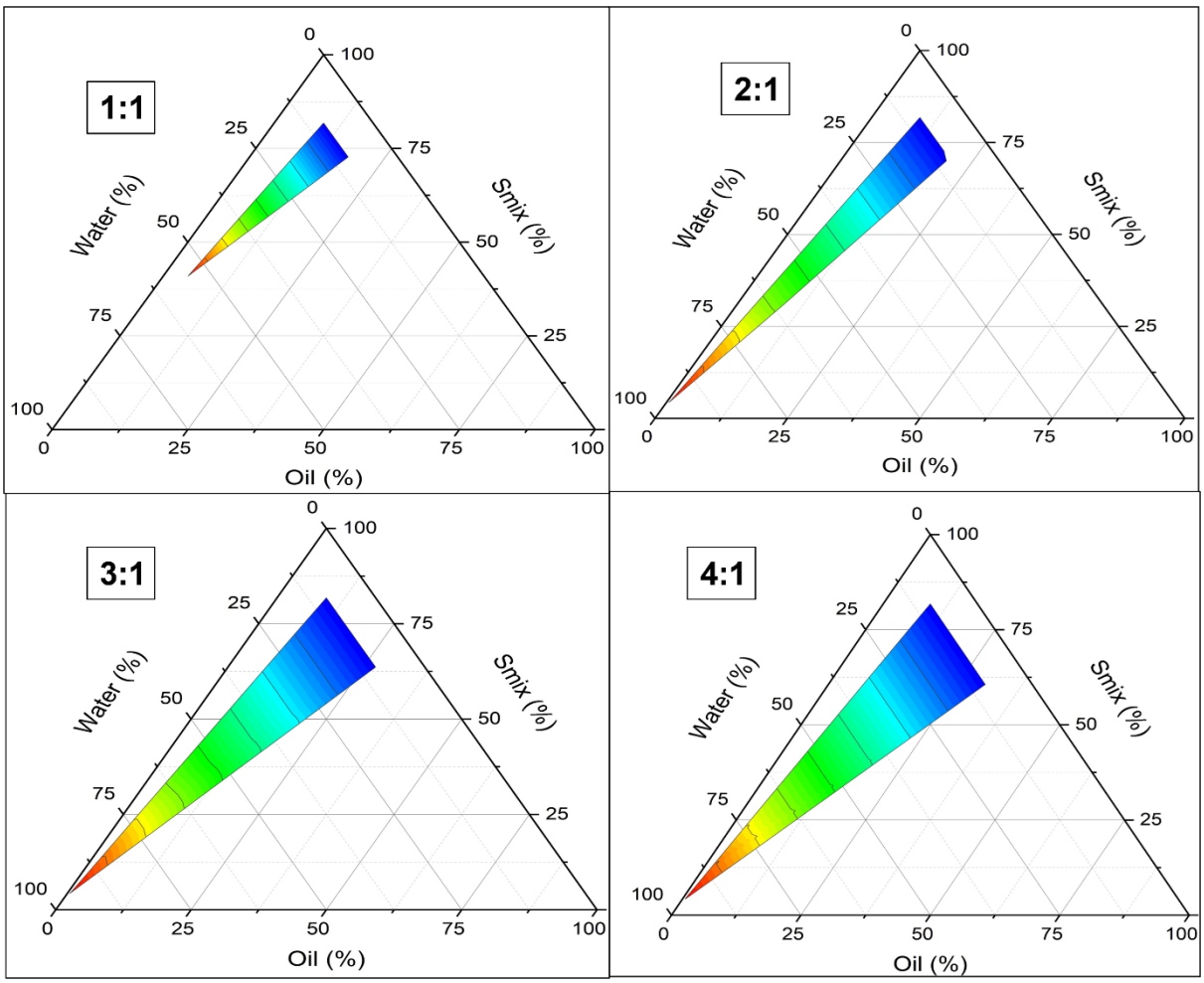

Figure 4. Pseudo-ternary phase diagram for different ratios of surfactant and co-surfactant.

2.5 Preparation of Placebo Nanoemulsion (NE) and its Optimization

Sixteen placebo NE were prepared with 4:1 S_{mix} to select the optimized ones. Five formulations were selected out of all based on clarity at the end of aqueous microtitration. Selected formulations were subjected to stress conditions viz thermodynamic and physical stability for further optimization. Table 1 represents the data of both the stability studies i.e., thermodynamic stability as well as physical stability. As per the data, two formulations show phase separation and are thus rejected (12).

Table 1. The outcome of stress conditions imposed on various formulations obtained from a pseudo-ternary phase diagram.

Formulation code	Smix ratio	Oil: Smix	Heating cooling cycle	Freeze thawing cycle	Centrifugation study	Result
NE1	4:1	1:9	-	-	-	Passed
NE2	4:1	1:5	+	+	+	Failed
NE3	4:1	1:6	-	+	+	Failed
NE4	4:1	1:7	-	-	-	Passed
NE5	4:1	1:8	-	-	-	Passed

(+) symbol represents the instability (turbidity/phase separation), whereas (-) symbol represents the absence of sign of instability

http://dx.doi.org/10.29228/jrp.144
J Res Pharm 2022; 26(3): 469-482

2.6 Characterization of Optimized nanoemulsion Formulation (4-MU-NE and MTO-NE)

2.6.1 Droplet size, polydispersity index (PDI), and percentage transmittance:

The average droplet size of MTO-NE was found to be in the range of 113.2 ± 5.3 nm to 173.8 ± 9.72 nm and for 4-MU in the range of 123.2 ± 6.17 nm to 177.3 ± 4.94 nm as depicted in Table 2.

The formulations PDI was determined to be 0.281 to 0.407 for MTO-NE and 0.254 to 0.395 for 4-MU-NE, signifying monomodal particle size distribution. The percent transmittance of MTO-NE was found to be in the range of 85.4 to 100 and for 4-MU-NE, it was 93.4 ± 0.73 to 98.8 ± 0.87.

2.6.2 Drug content and pH:

The percent drug content of MTO-NE was confirmed to be in the region of 97.39±2.37% to 98.42±3.14% while for 4-MU-NE, it was 97.71±2.07% to 98.48±4.61% as mentioned in Table 2. The % drug content denotes a proportion of the total amount of drugs included in the formulation. The pH of both formulations was found to be in the range of 5.3 to 5.5, values mentioned in Table 2.

Table 2. Characterization parameters for different MTO and 4-MU nanoemulsions.

Parameters	**4-MU NE1**	**4-MU-NE4**	**4-MU-NE5**	**MTO-NE1**	**MTO-NE4**	**MTO-NE5**
Particle Size	123.2±6.17	155.4±8.06	177.3±4.94	113.2±5.3	148.8±6.13	173.8±9.72
% Transmittance	98.02±0.32	96.9±0.22	95.8±0.87	98.8±1.07	97.3±0.3	93.4±0.73
PDI	0.254	0.323	0.395	0.281	0.372	0.407
Ph	5.3±0.53	5.5±0.39	5.5±0.46	5.4±0.64	5.5±0.74	5.3±0.35
Drug Content	97.13±2.82	98.48±4.61	97.71±2.07	98.42±3.14	97.39±2.37	98.01±3.98

2.6.3 In-vitro Drug Release Study

In vitro drug release of 4-MU-NEs was determined to be in the region of 61.88±4.267 % to 78.53±4.61 % in 8 h which was significantly higher as compared with 4-MU- Sus which was 33.854 ±6.0165 as displayed in Figure 6. The inadequate drug release of 4-MU-Sus might be attributed to the drug's inadequate solubility in water and buffers. The solubility of the 4-MU was enhanced by the preparation of nanoemulsion.

In vitro release study of MTO-NE was not performed because MTO is a water-soluble drug, and it is dissolved in the water phase of nanoemulsion. So, unlike 4-MU, there is no dissolution followed by the release of drug is expected. Rather, there would be quick diffusion of drugs across the dialysis membrane under the sink condition.

Based on the above characterization parameters, the rest of the nanoemulsion formulations were screened out and only MTO-NE1 and 4-MU-NE1 were taken forward for further study.

http://dx.doi.org/10.29228/jrp.144
J Res Pharm 2022; 26(3): 469-482

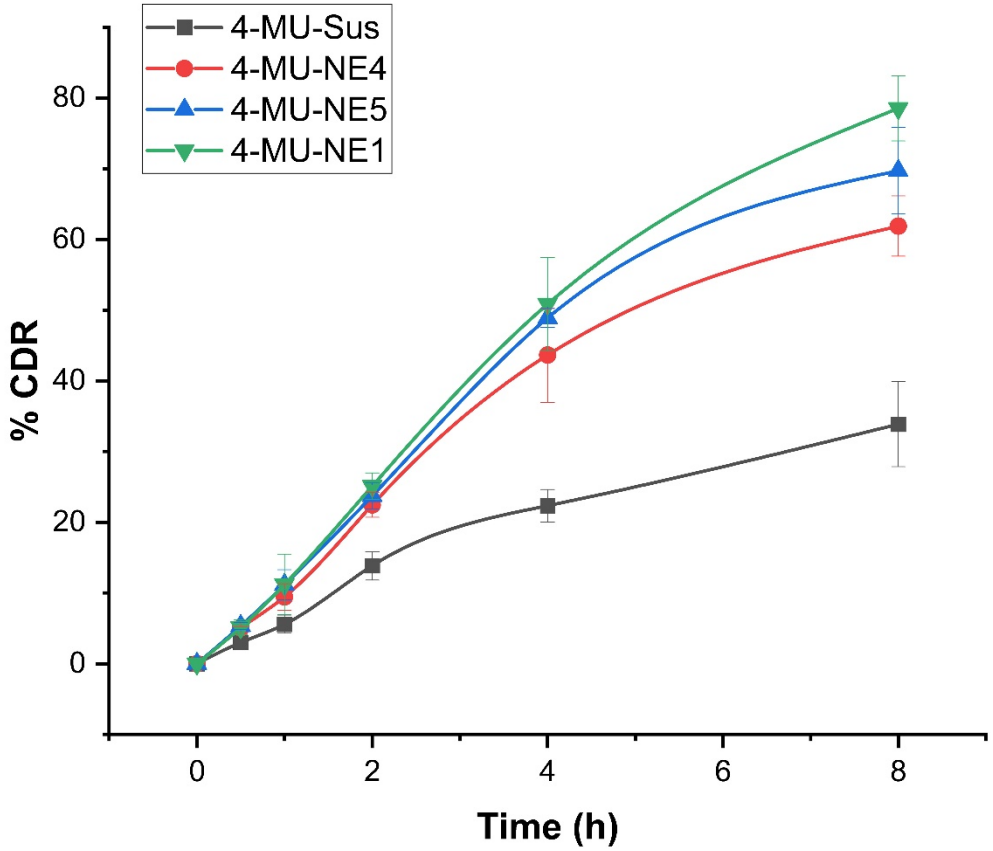

Figure 6. *In vitro* drug release pattern of 4-MU-NE

2.6.4 *Transmission electron microscopy (TEM):*

The TEM image of MTO-NE and 4-MU-NE is displayed in Figure 5. The NE droplets were found circular when examined by TEM. The size of the globules was ranging from 20nm to 200nm. The average size of the nanoparticles determined by TEM analysis conformed with the particle size determined previously by dynamic light scattering.

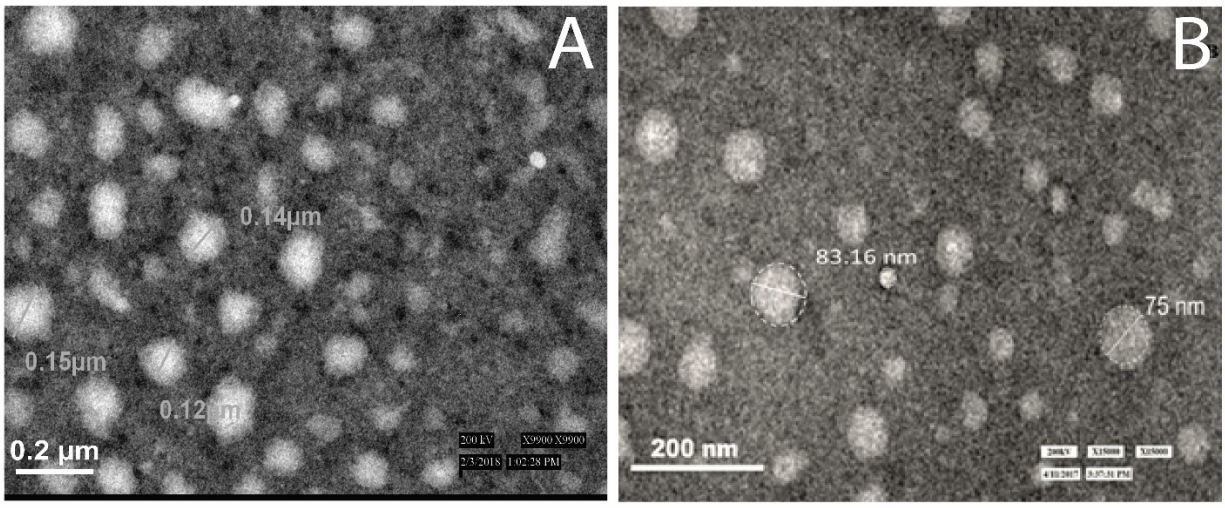

Figure 5. (A) TEM images of 4-MU-NE (B) TEM image of MTO-NE

http://dx.doi.org/10.29228/jrp.144
J Res Pharm 2022; 26(3): 469-482

2.7 Cytotoxicity Assay:

The impact of 4-MU, MTO, and their nanoemulsions on the viability of MCF-7 cells was assessed using the MTT test, which is shown in Figure 7. 4-MU, MTO, 4-MU-NE, and MTO-NE inhibited cell proliferation dose-dependently. The % cell viability of MCF-7 cells incubated with 4-MU and 4-MU-NE at tested concentrations ranging from 0.01-1mM for 72 hours was all over 95.54±2.88% to 56.96± 2.71 % for 4-MU and 93.48±3.70% to 45.72 ± 4.67 % for 4-MU-NE respectively, indicating that 4-MU-NE was found to have a significant effect on cell viability of MCF-7 cells with p-value 0.0226 (p-value <0.05) at the studied concentrations, implying that 4-MU-NE could be good biocompatible carriers for drug delivery.

Similarly, % cell viability for MTO and MTO-NE on MCF-7 cells was evaluated on different concentrations ranging from 0.1µM to 10µM for 72 h was found to be 91.62 ± 3.41% to 49.29 ± 2.96 % for MTO and 89.69 ± 7.63 % to 34.28 ± 5.06 % for MTO-NE respectively, which implies that MTO-NE was found to produce a significant effect on cell viability of MCF-7 cells with p-value 0.0115 (p-value <0.05).

The MTT test was used to analyze the cytotoxic impact of 4-MU and 4-MU-NE on the MCF-7 cell line, and the IC_{50} were 3.868 mM and 1.885 mM, respectively, against MCF-7. MTO and MTO-NE reported IC_{50} of 10.51 µM and 5.027 µM, respectively, against MCF-7.

The cytotoxicity of 4-MU-NE and MTO-NE was significantly higher than the 4-MU suspension and MTO solution respectively.

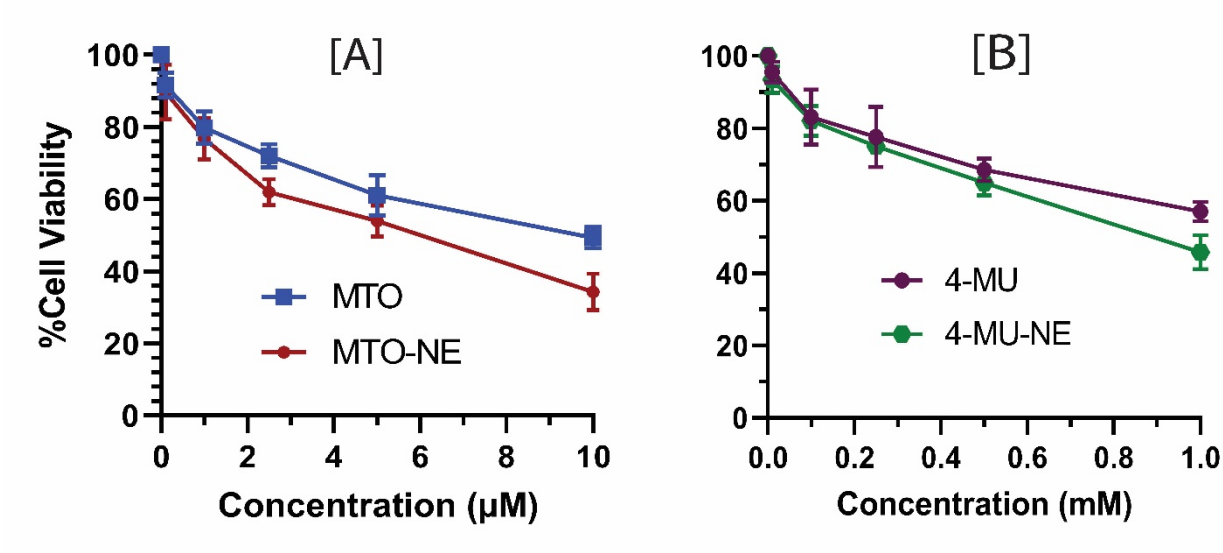

Figure 7. Comparison of % Cell viability activity; (A) MTO & MTO-NE (B) 4-MU & 4-MU-NE

3. DISCUSSION

The solubility of drugs was carried out in various oils (as shown in Figure 2) which were found to be helpful in the screening of oil based on the maximum solubility. As per the result obtained in selection of oil which is represented in figure 3, cinnamaldehyde was chosen as an internal phase for the NE formulation.(13). The explanation behind 4-MU's remarkable solubility in cinnamaldehyde may be attributed to the formation of H-bond which shows its ability to dissolve 4-MU to a greater extent. Also according to research paper by Liu et al. on cinnamaldehyde, it has been reported to have 59 potential targets in the therapy of breast cancer which can provide an additive effect with the drugs in the treatment of breast cancer (14).

Surfactant and cosurfactant screening were done based on oil solubilizing ability. According to the findings, tween 80 has the highest oil solubilizing ability, followed by tween 20 and PEG 400. To achieve good o/w NE the desirable HLB for Surfactant should be in between 8 to 18. Because of the highest oil solubilization and low molecular weight, Tween-80 decreases particle size better than polymeric surfactants (15). The ratio of surfactant and cosurfactant was calculated using a pseudo ternary phase diagram. Since phase diagrams with different ratios exhibited variable nanoemulsion areas, the 4:1 Smix ratio was chosen since it displayed the maximum nanoemulsion area as shown in Figure 4. As the surfactant and cosurfactant were tween 80 and PEG 400, Tween 80's greater HLB of 15.0 in contrast to PEG 400's HLB of 11.6 can be attributed to this enhancement in the nanoemulsion area. The increment of nanoemulsion region is attributed due to the

http://dx.doi.org/10.29228/jrp.144
J Res Pharm 2022; 26(3): 469-482

presence of a higher concentration of tween 80 as tween have higher HLB value i.e., 15 as compared to PEG 400 (12).

Placebo nanoemulsions were prepared in five different ratios of oil and S_{mix} i.e., 1:5, 1:6, 1:7. 1:8, 1:9 and subjected to various stress conditions i.e., freeze thaw cycle, heating cooling cycle and centrifugation for the assessment of their stability. The results revealed that two formulations were not able to pass the studies as their phase got separated due to the insufficient micelle formation between oil & S_{mix} as discussed in Table 1 (16). Thus, only three placebo formulations were carried forward to make chemotherapeutic loaded nanoemulsions. Based on the stability studies results obtained for placebo formulations, three separate formulations for both the drugs were prepared and further characterized for droplet size, PDI, percentage transmittance, drug content, pH and in vitro drug release studies as tabulated in Table 2. The results of droplet size indicate globules of chemotherapeutic formulation lies in the nano range revealing the optimum combination of oil and Smix. 4-MU-NE1 and MTO-NE1 shows minimum particle size along with minimum PDI which may be attributed to the maximum concentration of S_{mix} (1:9) employed (16). Percentage transmittance was also found to be greater for NE1 formulations. The % drug content denotes a proportion of the total amount of drugs included in the formulation which was greater for NE1 formulation. The reason may be the highest concentration of S_{mix} which solubilizes the maximum quantity of drug in the nanoemulsions (16). The pH of both formulations was found to be in the range of 5.3 to 5.5 which is as per the normal skin pH range (5.5–7.5). TEM studies of developed nanoemulsions represented in Figure 5, displayed circular globules, further confirming the nano size of optimized formulations.

In vitro release studies of 4-MU-NE displayed highest release of 78.53±4.61 % in 8 h as compared to 4-MU-Sus clearly depicted in Figure 6. This shows the sustained release behavior of 4-MU from the developed nanoemulsions.

A significant increase in the cytotoxicity on MCF-7 cells via MTT assay were observed for the MTO-NE and 4-MU-NE as compared to their respective free drug solution as represented in Figure 7. This may be attributed to the nano size of globules in drug loaded nanoemulsions which facilitated the entry of drug within the cells (17) and further cinnamaldehyde in the nanoemulsion composition enhanced the cytotoxic effect (14).

4. CONCLUSION

So far, a lot of research has been done to create effective anti-cancer nanoformulation to reduce unintended side effects of chemotherapeutics. In the current study, we created nanoemulsions of both the drugs 4-MU and MTO separately to precisely target MCF-7 cells and deliver the MTO and 4-MU molecules to the target cells. The chemical and physical stability of the nanoemulsions was confirmed in preliminary stability studies. *In vitro* drug release profile was enhanced using nanoemulsions. Finally, because of their improved water solubility, our novel nanoemulsion formulations of 4-MU and MTO may have the potential to lower the incidence and severity of breast cancer and increase bioavailability due to the decreased particle size. MCF-7 cells were treated with 4-MU-NE and MTO-NE, which exhibited anticancer activity. In comparison to free MTO and free 4-MU solutions, MTO-NE and 4-MU-NE demonstrated enhanced cytotoxicity in MCF-7 cells.

Overall, our findings suggest that nanoemulsions are effective carriers for the anticancer drugs MTO and 4-MU. On the other hand, *in-vivo* studies can be further carried out to assess the anticancer effects of the prepared formulations.

5. MATERIALS AND METHODS

5.1 Materials

Mitoxantrone (MTO) was bought from Cayman Chemicals, China. 4 -Methyl Umbelliferone (4-MU) and cinnamaldehyde oil were purchased from Sigma Aldrich, India, and Loba Chemie, India. Tween-80 and Polyethylene Glycol-400 (PEG 400) were purchased from Sisco Research Laboratory, Maharashtra, India. Liquid lipids viz all oils were procured from SD fine, India. The rest of the chemicals and solvents utilized were of analytical grade.

5.2 Experimental methods

5.2.1 Preformulation study for the selection of excipients

The choice of oil, surfactant, and co-surfactant was critical before formulation development. During the final excipient selection, the drug solubility parameters and the stability of the nanoemulsion were kept in mind.

http://dx.doi.org/10.29228/jrp.144
J Res Pharm 2022; 26(3): 469-482

Selection of Oil

For oil selection, the oils were chosen as per their ease of availability, such as Sesame oil, olive oil, liquid paraffin, castor oil, cinnamaldehyde, lemongrass oil, sunflower oil, oleic acid, and kalonji oil for the solubility of 4-MU. First 1ml of solvent (surfactant or oil) was poured a then large amount of drug was added. Using a Remi CM-101 cyclomixer it was then vortexed for 72 hours at room temperature (25±1 °C). Excess medication was removed from the mixture after 72 hours by centrifuging them at 3000 rpm for 10 minutes (Remi R8C Laboratory Centrifuge). In other MCT, 10 µl of supernatant was collected and methanol & water in a ratio of 1:1 was used to dilute it to 1 ml. Before filtering with a 0.22-micron nylon filter, the mixture was vortexed. After an appropriate dilution, the absorbance was measured at 320 nm, and the unknown amount of medication dissolved in that specific oil was estimated using a previously constructed calibration plot (13, 18).

Selection of Surfactant and Co-surfactant

The oil solubilizing ability of surfactants Tween 20, Tween 80, Span 20, Span80, PEG-400, PECOL, and Labrafac was tested during surfactant screening. To recapitulate, a 15% v/v surfactant solution was initially prepared in double-distilled water. After that, 5 µl of oil was added to the solution and vortexed vigorously on Remi CM-101 cyclomixer. The operation was repeated in the same way until the surfactant solution became turbid. (13)

Construction of pseudo-ternary phase diagram

Different S_{mix} ratios (1:3, 1:2, 1:1, 2:1, 3:1, 4:1) were evaluated, and the optimum surfactant-co-surfactant ratio was chosen based on its ability to create the largest nanoemulsion area in a pseudo ternary phase diagram. The ratio of Oil to S_{mix} was also adjusted to find the maximum Oil and lowest S_{mix} required to generate a nanoemulsion system(13)

In addition to the restraints (4-MU solubility in Oil and surfactant toxicity), varying the Oil: S_{mix} ratio helped to determine the lower and upper limits of Oil and S_{mix} concentration. These lower and upper bounds were meant to be used (19).

In brief, a homogeneous combination of Oil and S_{mix} was titrated stepwise with a certain amount of water, vortexed, and the resulting formulation was visually evaluated for turbidity or clarity. The transparent formulation symbolizes the nanoemulsion region, thus the Oil %, S_{mix} %, and water % required to generate a clear formulation at each stage were used to create a pseudo ternary phase diagram for a specified S_{mix} ratio (18).

Preparation of Placebo Nanoemulsion (NE) and its Optimization

The placebo nanoemulsion was made using the aqueous microtitration technique. Selected oil was placed in a 5 mL borosilicate glass container, S_{mix} was added, and the combination was vortexed until the oil and surfactant phases were miscible with one another. To make nanoemulsion, this mixture was titrated with a little amount of water (aqueous microtitration). The drug-loaded nanoemulsion for 4-MU was formed by dissolving 4-MU specific Oil and then followed by the same steps as the placebo nanoemulsion.

The nanoemulsion for MTO was prepared by dissolving MTO in water and preparing the nanoemulsion in the process as mentioned above(20).

5.2.2 Optimization based on Thermodynamic stability studies

The optimization of placebo NE was carried out by subjecting them to thermodynamic stability tests such as a freeze-thaw test and a heating-cooling cycle, as well as physical stability tests such as centrifugation, to reject metastable nanoemulsions (19).

Freeze-thaw study: The placebo nanoemulsions were kept at -18°C and 45°C for at least 48 hours in three separate cycles during this investigation.

Heating cooling study: This study followed the same specifications as the freeze-thaw study, with the exception that the lowest temperature in this test was –4°C. Six cycles were run for each formulation, with any differences being noted.

Physical stability studies via Centrifugation:

Using a Remi R8C Laboratory Centrifuge, the placebo nanoemulsion was centrifuged for 15 minutes at 5000 rpm (Mumbai, India). The nanoemulsions were observed for any signs of instabilities(12).

http://dx.doi.org/10.29228/jrp.144
J Res Pharm 2022; 26(3): 469-482

Preparation of optimized 4-MU Nanoemulsion (4-MU-NE) and MTO Nanoemulsion (MTO-NE)

The drug-loaded nanoemulsion for 4-MU was made by dissolving 4-MU in cinnamaldehyde followed by the same steps as mentioned for the placebo nanoemulsion. The nanoemulsion for MTO was prepared by dissolving MTO in water and preparing the nanoemulsion in the process as mentioned above.

Characterization of Optimized nanoemulsion Formulation (4-MU-NE and MTO-NE)

Droplet size, zeta potential, and polydispersity index (PDI).

Dynamic light scattering technique (Malvern Zetasizer, Nano ZS, UK) was utilized to determine the droplet size, zeta potential, and PDI of both formulated NEs. Before testing, 50 times dilution is done with all NE formulations and then the further study was done at 25°C at 90° angle of detection (21, 22).

Percentage transmittance and Refractive Index.

To have a better understanding of the size and stability of the globules of the created formulation, the percentage transmittance technique was applied. A UV–visible spectrophotometer was used to evaluate the percentage transmittance of both prepared formulations (Shimadzu, UV-1601, Kyoto, Japan) at 320 nm and 662 nm (Pathak et al., 2014). The formulation was not diluted, and double-distilled water was used as blank.

Drug content and pH.

Drug content was assessed by taking 1ml MTO NE (2mg/kg) equivalent of the drug. 10 µl of MTO-NE was used and 300 times dilution was done with methanol. After filtering through a nylon filter bearing a pore size of 0.22 µm diameter, the diluted MTO-NE was subjected to UV–visible spectrophotometer at 662 nm likewise 1ml of 4-MU-NE (20mg/kg) equivalent of equal was taken and the same procedure was followed at 320 nm. (Ahmed et al., 2018).

The following formula was used to determine the percentage of drug content:

$$\%\ Drug\ Content = \frac{Calculated\ amount\ of\ drug\ in\ Drug\ loaded\ NE}{\text{Initial amount of drug in Drug loaded NE}} x\ Dilution\ Factor\ x\ 100$$

The % drug content is a proportion of the total quantity of drug in the formulation. A previously calibrated pH meter was used to estimate the pH of MTO-NE and 4-MU-NE. The pH was obtained by dipping the glass electrode of a pH meter at room temperature directly into the sample (18, 23).

Transmission electron microscopy (TEM).

Transmission electron microscopy was used to examine the morphology of MTO-NE and 4-MU-NE at AIIMS in New Delhi, India. To assess morphology and size distribution first sample was diluted 50 times after that on the grid of copper a sample drop was placed using a micropipette. After 2 minutes, the copper grid was dried and immersed in 2% w/v phosphotungstic acid. The stained grids were then put on filter paper in a petri dish and CM 200, Philips Briarcliff Manor, NY, USA was used to examine them. (24) (25).

In vitro drug release

A dialysis membrane (MW 12,000–14,000) was used to conduct an *in vitro* drug release of the proposed formulation (Alam et al., 2018). Dissolution media comprises phosphate buffer (pH 6.4) and methanol in a ratio of 7:3 (Alexis et al., 2004). For *in vitro* studies of 4-MU suspension (4-MU-Sus) was formulated by suspending 4-MU in a 0.1 % carboxymethyl cellulose aqueous mixture. 0.5 ml samples of 4-MU-NE and 4-MU-Sus were added to the dialysis membrane. To prevent leakage, the membrane of both ends was sealed(26).

For 8 hours, the dialysis membrane was dipped in 50 ml of release media kept at 37 ±1 °C, and constantly stirred at 100 rpm. To maintain the sink condition, a 1 ml sample was taken from the release medium and replaced with a fresh 1 ml release medium at various periods (0.5, 1, 2, 3, 4, 6, and 8 h). At 320 nm (Shimadzu1800, Japan), 4-MU-NE samples were spectrophotometrically analyzed (20).

5.2.3 Cytotoxicity Assay

3-(4,5-Dimethylthiazol-2-yl)-2,5-Diphenyltetrazolium Bromide (MTT) test was used to investigate the cytotoxic potential of 4-MU and MTO on MCF-7 cell lines. In 100 µl of Dulbecco's Modified Eagle Medium (DMEM) and 10% Foetal bovine serum (FBS) MCF-7 cells ($1x10^3$ cells) were seeded in triplicate in 96-well microtiter plates and cultured for 24 h at 37°C in a CO_2 incubator(27). After the completion of 24 h, the medium was discarded and replaced with new media containing various doses of the 4-MU, 4-MU-NE, (0.01 mM to

http://dx.doi.org/10.29228/jrp.144
J Res Pharm 2022; 26(3): 469-482

1mM), MTO & MTO-NE(0.1µM to 10µM), which were incubated for 24 h at 37°C in a CO_2 incubator (28, 29). Each well had an ultimate volume of 100 µL. Upon completion of treatment, cells were rinsed with PBS, addition comes next of 10µl of MTT reagent and again incubated for 4 h in a CO_2 incubator at 37°C. After the incubation period had ended, the MTT reagent was withdrawn from each well, and 75 µL of dimethyl sulphoxide (DMSO) was pipetted into each well and carefully mixed(30, 31). Using a plate reader, the absorbance was measured at 540 nm, and the percentage of cell viability was determined using the formula %.

$$\%\ Cell\ Viability = \frac{Absorbance\ of\ treated\ cells}{Absorbance\ of\ control\ cells} x\ 100$$

Acknowledgements: The authors are thankful to Dr. Ashok K. Chauhan, Founder President, Ritnand Balved Education Foundation (RBEF), Amity Group of Institutions, for providing a research environment and facilities.

Author contributions: Author contributions: Concept – V.M., S.M.; Design – S.M., V.M.; Supervision – S.M., R.M.; Resource – V.M., A.G., N.J.; Materials – D.K., S.R.; Data Collection &/or Processing – V.M., A.G.; Analysis &/or Interpretation - V.M., S.R.; Literature Search – V.M., N.J.; Writing – V.M., N.J., A.G.; Critical Reviews – S.M., V.M., A.G., N.J., R.M., D.K., S.R.

Conflict of interest statement: The authors declared no conflict of interest.

REFERENCES

[1] Hayes A, Huang W, Yu J, Maisonpierre P, Liu A, Kern F, et al. Expression and function of angiopoietin-1 in breast cancer. Br J Cancer. 2000;83(9):1154-60. [CrossRef]
[2] Sung H, Ferlay J, Siegel RL, Laversanne M, Soerjomataram I, Jemal A, et al. Global cancer statistics 2020: GLOBOCAN estimates of incidence and mortality worldwide for 36 cancers in 185 countries. CA Cancer J Clin. 2021;71(3):209-49. [CrossRef]
[3] Verma D, Khuroo T, Talegaonkar S, Iqbal Z. Nanopotentiated combination cancer therapy: Chemotherapeutic and chemosensitizer (2C approach). Med Hypotheses. 2015;84(6):580-2. [CrossRef]
[4] Fang X, Cao J, Shen A. Advances in anti-breast cancer drugs and the application of nano-drug delivery systems in breast cancer therapy. J Drug Deliv Sci Technol. 2020;57:101662. [CrossRef]
[5] Bugde P, Biswas R, Merien F, Lu J, Liu D-X, Chen M, et al. The therapeutic potential of targeting ABC transporters to combat multi-drug resistance. Expert Opin Ther Targets. 2017;21(5):511-30. [CrossRef]
[6] Barar J, Kafil V, Majd MH, Barzegari A, Khani S, Johari-Ahar M, et al. Multifunctional mitoxantrone-conjugated magnetic nanosystem for targeted therapy of folate receptor-overexpressing malignant cells. J Nanobiotechnology. 2015;13(1):1-16. [CrossRef]
[7] Liu J, Ye Z, Xiang M, Chang B, Cui J, Ji T, et al. Functional extracellular vesicles engineered with lipid-grafted hyaluronic acid effectively reverse cancer drug resistance. Biomaterials. 2019;223:119475. [CrossRef]
[8] Yahya RS, El-Bindary AA, El-Mezayen HA, Abdelmasseh HM, Eissa MA. Biochemical evaluation of hyaluronic acid in breast cancer. Clin Lab. 2014;60(7):1115-21. [CrossRef]
[9] Karalis TT, Heldin P, Vynios DH, Neill T, Buraschi S, Iozzo RV, et al. Tumor-suppressive functions of 4-MU on breast cancer cells of different ER status: Regulation of hyaluronan/HAS2/CD44 and specific matrix effectors. Matrix Biol. 2019;78:118-38. [CrossRef]
[10] Lokeshwar VB, Lopez LE, Munoz D, Chi A, Shirodkar SP, Lokeshwar SD, et al. Antitumor activity of hyaluronic acid synthesis inhibitor 4-methylumbelliferone in prostate cancer cells. Cancer Res. 2010;70(7):2613-23. [CrossRef]
[11] Neubi GMN, Opoku-Damoah Y, Gu X, Han Y, Zhou J, Ding Y. Bio-inspired drug delivery systems: an emerging platform for targeted cancer therapy. Biomater Sci. 2018;6(5):958-73. [CrossRef]
[12] Iqbal R, Ahmed S, Jain GK, Vohora D. Design and development of letrozole nanoemulsion: A comparative evaluation of brain targeted nanoemulsion with free letrozole against status epilepticus and neurodegeneration in mice. Int J Pharm. 2019;565:20-32. [CrossRef]
[13] Azeem A, Rizwan M, Ahmad FJ, Iqbal Z, Khar RK, Aqil M, et al. Nanoemulsion components screening and selection: a technical note. AAPS PharmSciTech. 2009;10(1):69-76. [CrossRef]
[14] Liu Y, An T, Wan D, Yu B, Fan Y, Pei X. Targets and mechanism used by cinnamaldehyde, the main active ingredient in cinnamon, in the treatment of breast cancer. Front Pharmacol. 2020;11:1751. [CrossRef]
[15] Ghosh V, Mukherjee A, Chandrasekaran N. Ultrasonic emulsification of food-grade nanoemulsion formulation and evaluation of its bactericidal activity. Ultrason Sonochem. 2013;20(1):338-44. [CrossRef]
[16] Georgiev MT, Aleksova LA, Kralchevsky PA, Danov KD. Phase separation of saturated micellar network and its potential applications for nanoemulsification. Colloids Surf Physicochem Eng Aspects. 2020;607:125487. [CrossRef]
[17] Alkhatib MH, AlBishi HM. In vitro evaluation of antitumor activity of doxorubicin-loaded nanoemulsion in MCF-7 human breast cancer cells. J Nanopart Res. 2013;15(3):1-15. [CrossRef]

[18] Gull A, Ahmed S, Ahmad FJ, Nagaich U, Chandra A. Effect of polyherbal microemulsion on Staphylococcus epidermidis: Formulation development, CCD based optimization, characterization, and antibacterial activity by scanning electron microscopy. J Drug Deliv Sci Technol. 2020;57:101641. [CrossRef]
[19] Iqbal R, Ahmed S, Jain GK, Vohora D. Design and development of letrozole nanoemulsion: A comparative evaluation of brain targeted nanoemulsion with free letrozole against status epilepticus and neurodegeneration in mice. Int J Pharm. 2019;565:20-32. [CrossRef]
[20] Ahmed S, Gull A, Alam M, Aqil M, Sultana Y. Ultrasonically tailored, chemically engineered and "QbD" enabled fabrication of agomelatine nanoemulsion; optimization, characterization, ex-vivo permeation and stability study. Ultrason Sonochem. 2018;41:213-26. [CrossRef]
[21] Nagaich U, Gulati N. Nanostructured lipid carriers (NLC) based controlled release topical gel of clobetasol propionate: design and in vivo characterization. Drug Deliv Transl Res. 2016;6(3):289-98. [CrossRef]
[22] Kumar S, Ali J, Baboota S. Design Expert® supported optimization and predictive analysis of selegiline nanoemulsion via the olfactory region with enhanced behavioural performance in Parkinson's disease. Nanotechnology. 2016;27(43):435101. [CrossRef]
[23] Gulati N, Nagaich U, Saraf SA. Intranasal delivery of chitosan nanoparticles for migraine therapy. Sci Pharm. 2013;81(3):843-54. [CrossRef]
[24] Kawish S, Ahmed S, Gull A, Aslam M, Pandit J, Aqil M, et al. Development of nabumetone loaded lipid nano-scaffold for the effective oral delivery; optimization, characterization, drug release and pharmacodynamic study. J Mol Liq. 2017;231:514-22. [CrossRef]
[25] Ahmed S, Gull A, Aqil M, Ansari MD, Sultana Y. Poloxamer-407 thickened lipid colloidal system of agomelatine for brain targeting: Characterization, brain pharmacokinetic study and behavioral study on Wistar rats. Colloids Surf B Biointerfaces. 2019;181:426-36. [CrossRef]
[26] Khuroo T, Verma D, Khuroo A, Ali A, Iqbal Z. Simultaneous delivery of paclitaxel and erlotinib from dual drug loaded PLGA nanoparticles: Formulation development, thorough optimization and in vitro release. J Mol Liq. 2018;257:52-68. [CrossRef]
[27] Verma D, Thakur PS, Padhi S, Khuroo T, Talegaonkar S, Iqbal Z. Design expert assisted nanoformulation design for co-delivery of topotecan and thymoquinone: Optimization, in vitro characterization and stability assessment. J Mol Liq. 2017;242:382-94. [CrossRef]
[28] Anzar N, Mirza MA, Anwer K, Khuroo T, Alshetaili AS, Alshahrani SM, et al. Preparation, evaluation and pharmacokinetic studies of spray dried PLGA polymeric submicron particles of simvastatin for the effective treatment of breast cancer. J Mol Liq. 2018;249:609-16. [CrossRef]
[29] Khuroo T, Verma D, Talegaonkar S, Padhi S, Panda AK, Iqbal Z. Topotecan–tamoxifen duple PLGA polymeric nanoparticles: investigation of in vitro, in vivo and cellular uptake potential. Int J Pharm. 2014;473(1-2):384-94. [CrossRef]
[30] Padhi S, Mirza MA, Verma D, Khuroo T, Panda AK, Talegaonkar S, et al. Revisiting the nanoformulation design approach for effective delivery of topotecan in its stable form: An appraisal of its in vitro Behavior and tumor amelioration potential. Drug Deliv. 2016;23(8):2827-37. [CrossRef]
[31] A Ansari K, J Torne S, Vavia PR, Trotta F, Cavalli R. Paclitaxel loaded nanosponges: in-vitro characterization and cytotoxicity study on MCF-7 cell line culture. Curr Drug Del. 2011;8(2):194-202. [CrossRef]

http://dx.doi.org/10.29228/jrp.144
J Res Pharm 2022; 26(3): 469-482